OXFORD

DDRGK1 is required for the proper development and maintenance of the growth plate cartilage

Monika Weisz-Hubshman (iD), Adetutu T. Egunsula, Brian Dawson, Alexis Castellon, Ming-Ming Jiang, Yuqing Chen-Evenson,

Yu Zhiyin, Brendan Lee and Yangjin Bae*

Department of Molecular and Human Genetics, Baylor College of Medicine, Houston, TX 77030, USA
*To whom correspondence should be addressed at: Department of Molecular and Human Genetics, Baylor College of Medicine, One Baylor Plaza, Room R816,
Houston, TX 77030, USA. Tel: +1 7137984572; Email: bae@bcm.edu

Abstract

Loss-of-function mutations in *DDRGK1* have been shown to cause Shohat type spondyloepimetaphyseal dysplasia (SEMD). In zebrafish, loss of function of *ddrgk1* leads to defects in early cartilage development. *Ddrgk1*$^{-/-}$ mice show delayed mesenchymal condensation in the limb buds and early embryonic lethality. Mechanistically, Ddrgk1 interacts with Sox9 and reduces ubiquitin-mediated proteasomal degradation of Sox9 protein. To investigate the cartilage-specific role of *DDRGK1*, conditional knockout mice were generated by intercrossing *Prx1-Cre* transgenic mice with *Ddrgk*$^{fl/fl}$ mice to delete its expression in limb mesenchymal cells. Mutant mice showed progressive severe shortening of the limbs and joint abnormalities. The growth plate showed disorganization with shortened proliferative zone and enlarged hypertrophic zone. In correlation with these findings, Sox9 and Col2a1 protein levels were decreased, while Col10a1 expression was expanded. These data demonstrate the importance of Ddrgk1 during growth plate development. In contrast, deletion of *Ddrgk1* with the osteoblast-specific *Osteocalcin-Cre and Leptin receptor-Cre* lines did not show bone phenotypes, suggesting that the effect on limb development is cartilage-specific. To evaluate the role of *DDRGK1* in cartilage postnatal homeostasis, inducible *Agc1-Cre*^{ERT2}; *Ddrgkl*$^{fl/fl}$ mice were generated. Mice in which *Ddrgk1* was deleted at 3 months of age showed disorganized growth plate, with significant reduction in proteoglycan deposition. These data demonstrate a postnatal requirement for Ddrgk1 in maintaining normal growth plate morphology. Together, these findings highlight the physiological role of Ddrgk1 in the development and maintenance of the growth plate cartilage. Furthermore, these genetic mouse models recapitulate the clinical phenotype of short stature and joint abnormalities observed in patients with Shohat type SEMD.

Graphical Abstract
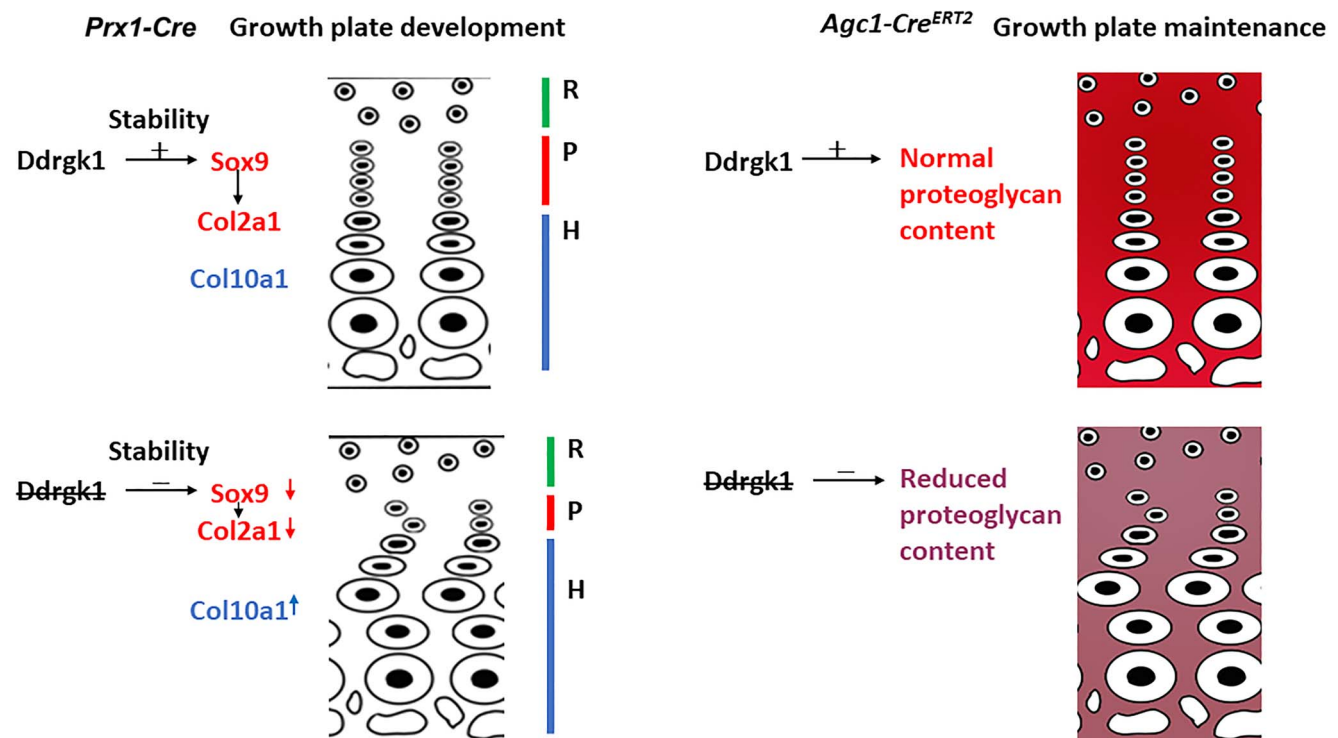
Introduction

Spondyloepimetaphyseal dysplasia (SEMD) is a group of heterogeneous skeletal dysplasia, associated with developmental abnormalities of the spine, epiphysis and metaphysis (1,2). The hallmark of the SEMD is disproportionate short stature. Extra-skeletal features and early onset osteoarthritis are frequently associated with SEMD (3). The genetic causes are variable and can affect extracellular matrix proteins (ECMs), protein transport, protein processing and post-translational modifications (PTMs) of ECMs.

UFM1 modification (ufmylation) is an ubiquitin-like PTM, mediated by the cascade function of specific E1 (UBA5)-E2 (UFC1)-E3 (UFL1)-like enzymes (4). During the ufmylation process, UFM1 (ubiquitin fold modifier 1) is attached covalently to its substrate after its maturation. De-ufmylation (UFM1 removal) and UFM1 maturation are mediated by two unique cysteine proteases called UFSP1 and UFSP2 (5). The function of ufmylation process is still poorly understood (6,7) and the physiological role of ufmylation in chondrogenesis has not been systematically explored. Many studies suggest important role for ubiquitination and ubiquitin-like modification in skeletal homeostasis and chondrogenesis (6,7). For example, ubiquitination of AXIN has been shown to be associated with induction of the Wnt canonical pathway and chondrocyte apoptosis in osteoarthritis (8). SOX9, the master transcription factor in chondrogenesis, undergoes ubiquitination and proteasomal degradation as previously reported (7,9,10). In addition, SOX9 has been shown to undergo multiple other types of post-translational modifications, which regulate its function including phosphorylation (11), acetylation (12,13) and sumoylation, another type of ubiquitin-like modification (14,15). In recent years, our group and others reported mutations in regulators of the ufmylation process that were associated with skeletal dysplasia (9,16,17). *UFSP2* mutations have been shown to cause hip dysplasia and SEMD with variable severity inherited in an autosomal dominant manner (16–18). Previously, we have demonstrated that loss-of-function mutations in *DDRGK1* were associated with Shohat type SEMD (9,19).

DDRGK1 (UFBP1, C20orf116), the first ufmylation substrate described, is ufmylated through interaction with UFL1, the only E3 known for ufmylation (5). DDRGK1 is de-ufmylated by UFSP2, at the ER membrane, the main compartment in which DDRGK1 is localized (20,21). In previous *in vivo* studies, *ddrgk1* knockdown in zebrafish resulted in defects in craniofacial cartilage. These cartilage abnormalities were rescued both by *ddrgk1* and *sox9* mRNA injection, and furthermore, these studies suggested that *sox9* functions downstream to *ddrgk1*. *Ddrgk1* knockout mice are early embryonic lethal. Interestingly, at E11.5, the *Ddrgk1* knockout mice showed delayed mesenchymal condensation in the limb buds in association with decreased Sox9 protein levels. The interaction between SOX9 and DDRGK1 was further confirmed *in vitro*, where DDRGK1 was found to stabilize SOX9 protein

levels by reducing its ubiquitination and its proteasomal degradation (9). These results indicated that DDRGK1 has an important role in SOX9 regulation and prompted further studies on DDRGK1 role in cartilage development and homeostasis.

In this study, DDRGK1's requirement in growth plate development as well as in postnatal growth plate homeostasis was demonstrated by the utilization of conditional knockout (cko) mouse models. *Ddrgk1* was deleted in early limb mesenchymal cells by using *Prx1-Cre* mouse line to investigate its role in chondrogenesis during embryonic development and then in postnatal cartilage by using the inducible *Agc1-Cre*^{ERT2} mouse line.

Results

Deletion of *Ddrgk1* in early mesenchymal cells (*Prx1-Cre; Ddrgk1*$^{fl/fl}$) causes severe limb shortening and deformation in mice

Since global knockout of *Ddrgk1* is embryonic lethal between E11.5 and E12.5 (9), the *Prx1-Cre*-driven cko (Prx1-cko) line was used to understand the physiological role of Ddrgk1 in early limb development and chondrogenesis. The cko mice showed severe shortening of limbs with blunted growth as indicated by weight (Fig. 1). The phenotypic findings worsened with age and cko mice developed severe joint deformities (Supplementary Material, Fig. S1A) and failure to thrive. The cko mice had delayed epiphyseal development and joint dislocations (Fig. 1B, Supplementary Material, Fig. S1A). Based on the micro-CT analysis at 8 weeks postpartum, bowing of the long bones was observed with reduced trabecular bone and cortical bone volume (Fig. 2A and B). The delay in epiphyseal development and reduced trabecular bone was confirmed by Van-Kossa staining at 8 weeks of age (Fig. 2C). Efficient *Ddrgk1* deletion was detected at the genomic DNA and mRNA levels (Supplementary Material, Fig. S1B and C). Since conditional deletion of *Ddrgk1* in mesenchymal cells led to bone deformities and low bone mass, Ddrgk1's role in osteogenesis was further evaluated utilizing the Osteocalcin-Cre (*OC-Cre*) conditional mouse line (22) in which *Ddrgk1* was deleted in mature osteoblastic lineage. The *OC-Cre; Ddrgk1*$^{fl/fl}$ mice were comparable in size and growth to *Ddrgk1*$^{fl/fl}$ control mice (data not shown). In addition, no significant changes in bone volume of the *OC-Cre; Ddrgk1*$^{fl/fl}$ in comparison with the control mice were observed at 8 weeks of age (Fig. 3A and B). We performed *in vitro* osteoblast differentiation assay using bone marrow stromal cells derived from *OC-Cre; Ddrgk1*$^{fl/fl}$ and *Ddrgk1*$^{fl/fl}$ mice to compare osteogenic differentiation ability. We did not find differences between the cko mice and the control mice (Fig. 3C). To further substantiate our findings, we evaluated Ddrgk1's role in osteogenesis by using the Leptin receptor-Cre (*Lepr-Cre*) conditional mouse line (23) where *Ddrgk1* was deleted in osteogenic progenitors (24,25). Similar to *OC-Cre; Ddrgk1*$^{fl/fl}$ mice, the *Lepr-Cre; Ddrgk1*$^{fl/fl}$ showed no difference in size and
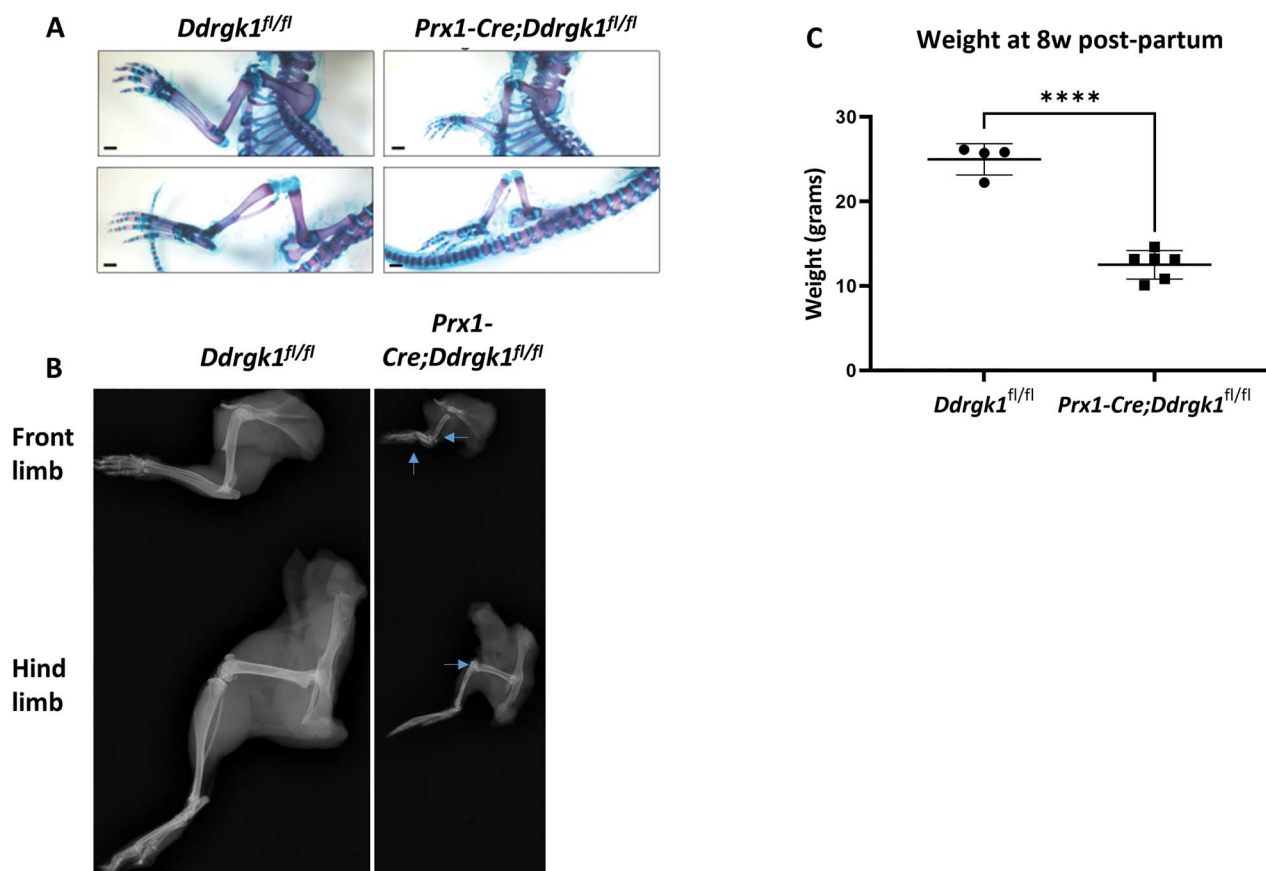
Figure 1. Conditional deletion of *Ddrgk1* in *Prx1-Cre* mice causes severe limb anomalies. (**A**) Alcian blue and Alizarin red staining of skeletal preparations at P7. Scale bars, 0.1 cm. (**B**) X-ray images of 8–week-old mice showing severe shortening of long bones as well as joint deformities of elbow, radio-carpal joint and knees (blue arrows). (**C**) Weight comparison in males at 8 weeks postpartum. Student's *t*-test was used for statistical analysis. ****$P < 0.0001$. N = between 3 and 6 mice.

growth to *Ddrgk1*$^{fl/fl}$ control mice. Micro-CT evaluation of bone volume at 8 weeks of age did not show any significant differences between the *Lepr-Cre; Ddrgk1*$^{fl/fl}$ and control *Ddrgk1*$^{fl/fl}$ mice (Fig. 4A and B). Collectively, these results suggest that Ddrgk1 is not required for osteoblastogenesis and that the reduced bone volume observed in the *Prx1-Cre* model may be secondary effect to the severe abnormalities in chondrogenesis and not a primary bone defect.

Prx1-Cre; Ddrgk1$^{fl/fl}$ cko mice have abnormal growth plate development

To further evaluate the cartilage abnormalities in the *Prx1*-cko mice, hematoxylin and eosin (H&E) staining was performed on growth plates of P2 mice in comparison with growth plate of control *Ddrgk1*$^{fl/fl}$ mice. The H&E staining showed severe abnormalities of growth plate organization with loss of the columnar organization of the proliferating zone as well as shortening of the proliferating zone in the cko mice (Fig. 5A and B). In addition, the hypertrophic zone of the growth plate in cko mice was expanded when compared to *Ddrgk1*$^{fl/fl}$ control mice (Fig. 5A and B). This finding was further supported by Col10a1 immunofluorescent staining, a hypertrophic chondrocyte marker as shown in Figure 5C.

This histological result corroborates with the progressive shortening of the limb in cko mice (Fig. 1), suggesting the critical role of *Ddrgk1* in proper growth plate organization during development.

Growth plate abnormalities in the *Prx1-Cre; Ddrgk1*$^{fl/fl}$ mice are associated with reduced protein expression of Sox9 and Col2a1

Immunofluorescence staining was performed to assess the protein level of chondrogenic markers including Sox9 and its downstream target Col2a1. Sox9 expression was reduced in the proliferating and prehypertrophic zones (Fig. 6A), while Col2a1 expression was reduced in the resting and proliferating regions at P2 (Fig. 6B). These results confirm that Ddrgk1 is an upstream regulator of Sox9 during cartilage differentiation and are consistent with previous findings on Sox9 expression pattern in the developing growth plate (26).

Postnatal deletion of Ddrgk1 (*Agc1-Cre*^{ERT2}; *Ddrgk1*$^{fl/fl}$) causes growth plate abnormalities and reduced proteoglycan content

To assess whether Ddrgk1 has a role in postnatal cartilage maintenance, *Agc1-Cre*^{ERT2}-inducible mouse model was used. At 3 months of age, *Agc1-Cre*^{ERT2}; *Ddrgk1*$^{fl/fl}$
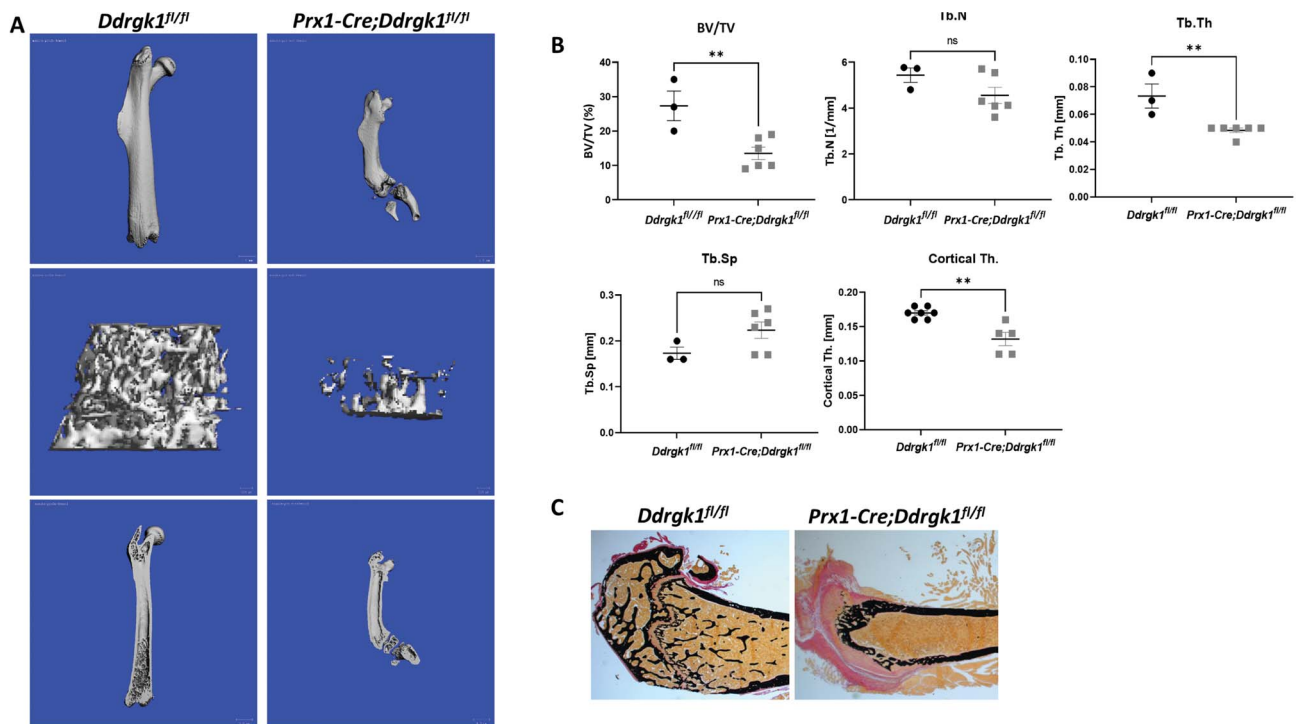
Figure 2. Mesenchymal conditional deletion of *Ddrgk1* is associated with low bone mass in adult mice and abnormal epiphyseal formation. (**A**) Micro-CT images and analysis of femurs at 8-week-old male mice, left panel—3D model of scanned bone showing severe long bone shortening and bowing. (**B**) Quantification of micro-CT analysis—trabecular bone and cortical bone in femurs ($n = 3$–7). Asterisk denotes significant change $P < 0.05$. (**C**) Van-Kossa staining of long bones in male mice at 8 weeks shows reduced mineralization and trabecular bone in *Prx1-Cre; Ddrgk1*$^{fl/fl}$ mice as well absence of secondary ossification center at 8 weeks postpartum. Scale 50 microns.

mice were treated with tamoxifen for 5 days and collected at 6 months of age. The deletion of *Ddrgk1* in chondrocytes was confirmed by immunohistochemistry that showed marginal detection of Ddrgk1 protein in chondrocytes of the growth plate (Fig. 7A). The growth plate of *Agc1-Cre*^{ERT2}; *Ddrgk1*$^{fl/fl}$ on H&E staining showed abnormal chondrocytes morphology compared to the *Ddrgk1*$^{fl/fl}$ in addition to its widening and disorganization (Fig. 7B). The growth plate chondrocytes showed rounded morphology with an enlarged cytoplasm compared to *Ddrgk1*$^{fl/fl}$. Changes in Col2a1 expression in the growth plates were not observed (Fig. 7C). Based on Safranin O staining, a significant decrease in the proteoglycan content was seen in the growth plate of *Agc1-Cre*^{ERT2}; *Ddrgk1*$^{fl/fl}$ (Fig. 7D). Similarly, reduced proteoglycan staining was observed in *Sox9* postnatal inducible deletion by *Agc1-Cre*^{ERT2} mouse model (27).

The results of the cko mouse studies suggest that Ddrgk1 has a key role in both chondrogenesis and chondrocyte homeostasis and partially phenocopies the outcome of cko of *Sox9* in both *Prx1-Cre* and *Agc1-Cre* models (26,27). The previously published results with the results of the current study further support the requirement of a Ddrgk1-Sox9 interaction during cartilage development.

Discussion

Chondrogenesis is a critical process for the development, growth and maintenance of a healthy skeleton.

It requires orderly differentiation of chondrocytes in a tightly regulated spatial and temporal fashion. Dysregulation of the cellular and molecular mechanisms that govern chondrogenesis leads to the development of various types of skeletal dysplasia (1). PTMs are versatile tools in cellular regulation and have important role in many physiological and pathological conditions (28,29). Ubiquitination and ubiquitin-like modifications are considered the most frequent PTMs after phosphorylation and glycosylation (28).

DDRGK1 is an ufmylation substrate as well as ufmylation process regulator through its binding to UFL1 (5). Loss-of-function mutations in *DDRGK1* were identified as a cause of Shohat type SEMD. Global knockout of *Ddrgk1*is lethal in mice between E11.5 and E12.5 (9); thus, to investigate further the function of *Ddrgk1* in chondrogenesis and cartilage homeostasis, the conditional *Prx1-Cre* mouse model was used to knockout *Ddrgk1* in early limb mesenchymal cells. The results showed severe cartilage developmental abnormalities in mice with severe long bone shortening and progressive joint deformities as observed in Shohat type SEMD (Fig. 1 and Supplementary Material, Fig. S1). Similar to the cko of Sox9 in mesenchymal cells (26), bone abnormalities were observed in the *Prx1-Cre; Ddrgk1*$^{fl/fl}$ mice including a delay in secondary ossification center formation as well as bowing of the bones (Fig. 2). The phenotype was significantly less severe than the conditional Sox9 knockout in which there was a severe impairment in bone formation;
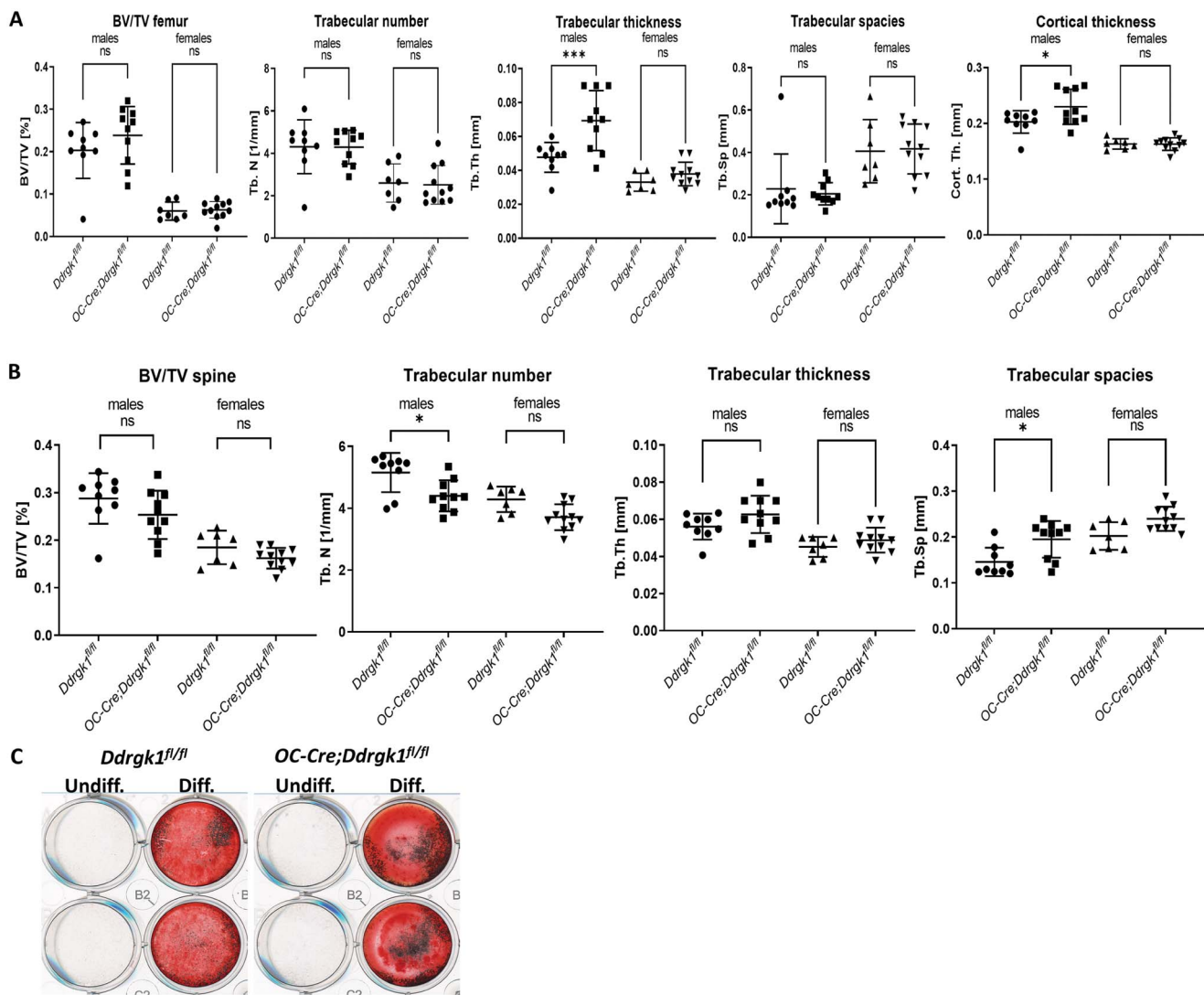
Figure 3. Quantification of micro-CT results of femurs (**A**) and spines (**B**) of males and females of *OC-Cre; Ddrgk1^{fl/fl}* mice at 8 weeks of age compared to control *Ddrgk1^{fl/fl}* mice. *$P < 0.05$, ***$P < 0.001$. $N = 7–9$ mice. (**C**) *In vitro* osteogenic differentiation of bone marrow stromal cells from *OC-Cre; Ddrgk1^{fl/fl}* mice and control *Ddrgk1^{fl/fl}* mice. $N − 1$, male from each genotype, with technical duplicate.

thus, the bone phenotype was further assessed with the use of osteoblast-specific *OC-Cre* mouse line and *Lepr-Cre* mouse line, which showed that Ddrgk1 did not have a primary function during osteogenesis (Figs 3A–C and 4A and B). These findings are also in line with the clinical phenotype of the Shohat type SEMD patients who do not exhibit bone fragility or reduced bone mass.

The long bone shortening and joint abnormalities of the *Prx1-Cre; Ddrgk1^{fl/fl}* mice were accompanied by abnormal growth plate organization with widened hypertrophic zone associated with increased Col10a1 expression and reduced, disorganized proliferating zone (Fig. 5). Based on the immunohistochemical analysis of the growth plate, reduced Sox9 and Col2a1 protein expression were seen confirming the results of our previous studies in which DDRGK1 regulated SOX9 protein stability (9) (Fig. 6). Downregulation of Col2a1 protein, one of main Sox9 downstream targets, further

supports the role of Ddrgk1 in chondrogenesis and its molecular function in Sox9 regulation. Deletion of *Sox9* in limb bud mesenchymal cells (*Prx1-Cre* mouse model) is lethal in the immediate postnatal period due to respiratory insufficiency (26). *Ddrgk1* conditional deletion in the same mouse model is not lethal and no respiratory problems were observed but the survival of these mice was reduced due to failure to thrive (data not shown). Although Sox9 protein level reduction was observed, the deletion efficiency of Ddrgk1 was incomplete, which could explain the remaining Sox9 protein expression and the absence of lethality. The growth plate abnormalities including decrease in proliferative zone and expansion of the hypertrophic zone are in concordance with the reduction in Sox9 expression. Sox9 regulates chondrocyte proliferation and delays hypertrophy (26) of chondrocytes; thus, reduction in Sox9 protein level would change this balance toward an increase in hypertrophic chondrocytes and reduced proliferative chondrocytes.
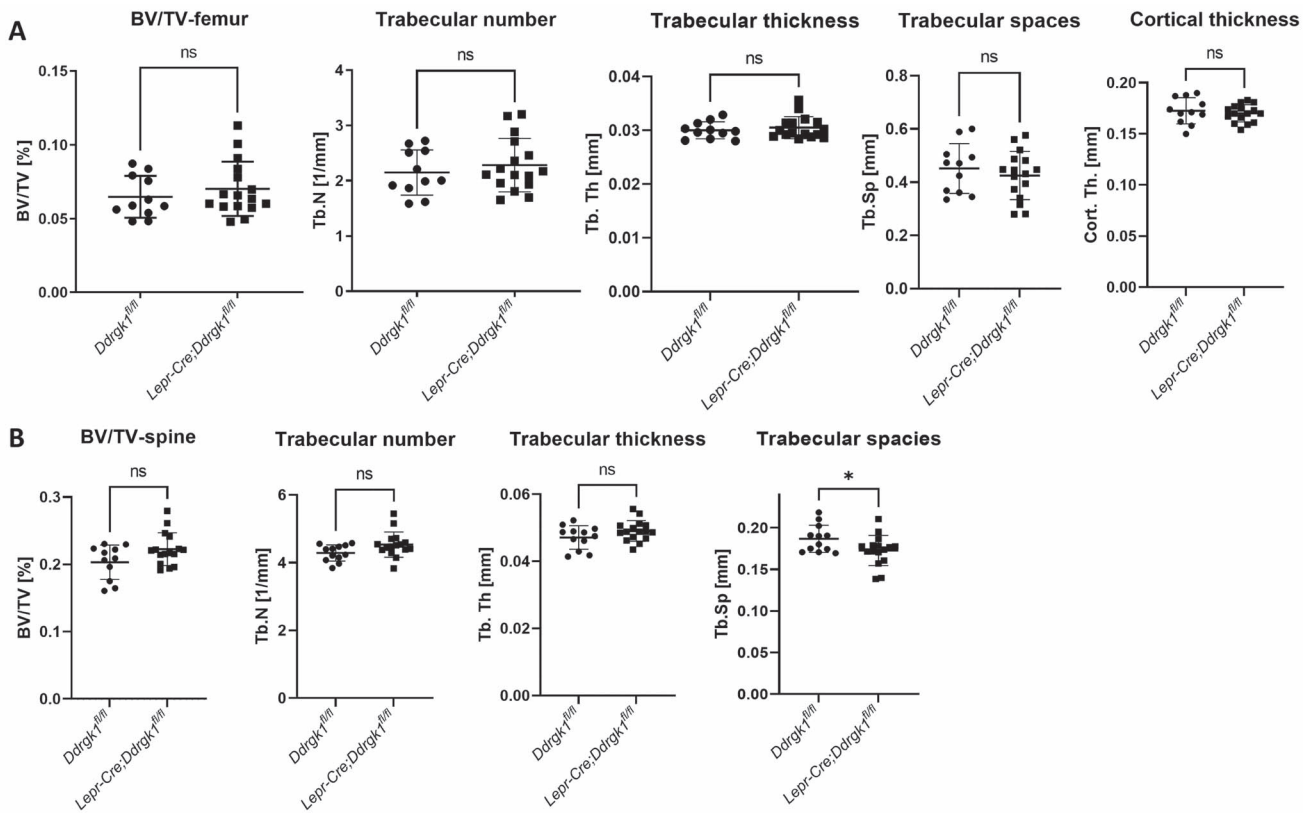
Figure 4. Quantification of micro-CT results of femurs (**A**) and spines (**B**) of female *Lepr-Cre; Ddrgk1^{fl/fl}* mice at 8 weeks of age compared to control *Ddrgk1^{fl/fl}* mice. *$P < 0.05$. $N = 11$–16 mice.
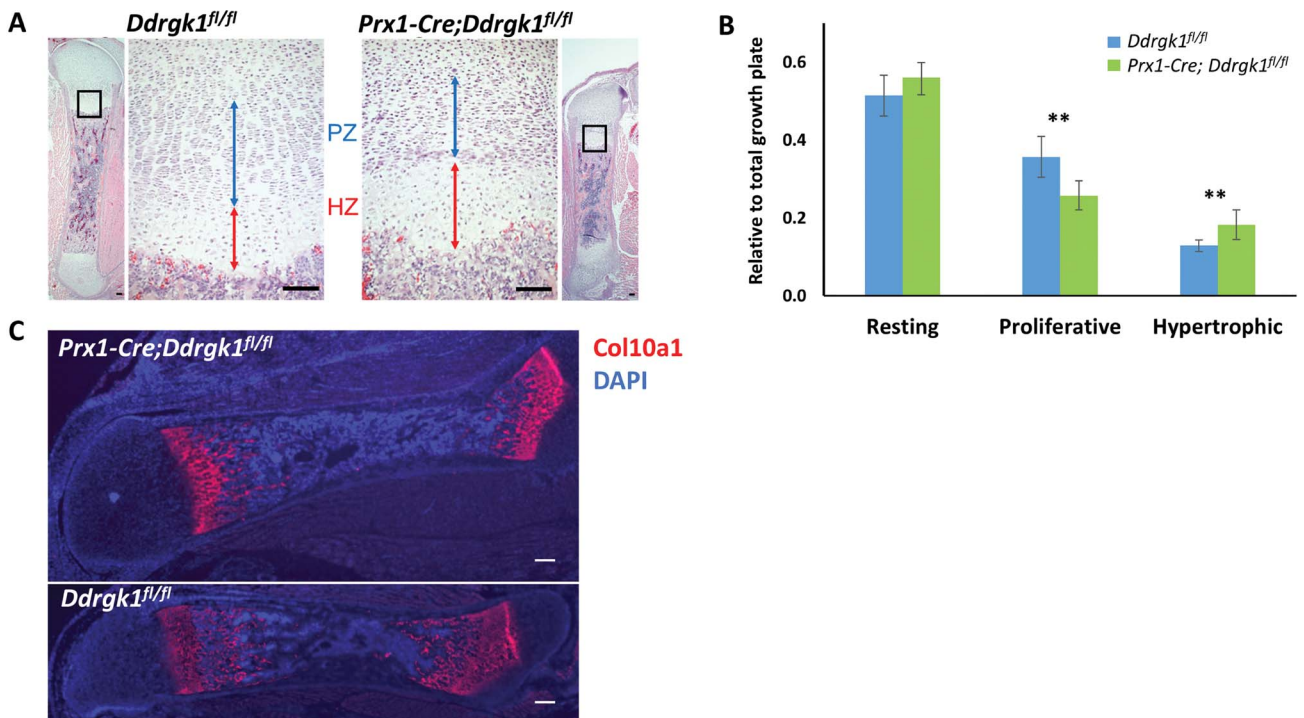

Figure 5. Deletion of *Ddrgk1* causes abnormal growth plate organization. (**A**) *Prx1-Cre; Ddrgk1^{fl/fl}* mice show a shortened proliferating zone (PZ) but elongated hypertrophic zone (HZ). The chondrocytes within *Prx1-Cre; Ddrgk1^{fl/fl}* mice growth plate are disorganized. H&E-stained femurs at P2. Scale bars, 100 μM. (**B**) Quantification of each zone, $n = 6$–7. Values represented as means $\pm$ SEM (**$P < 0.01$ two-tailed *t*-test). (**C**) Immunofluorescence staining of Col10a1 of hypertrophic zone. Scale 50 micron.
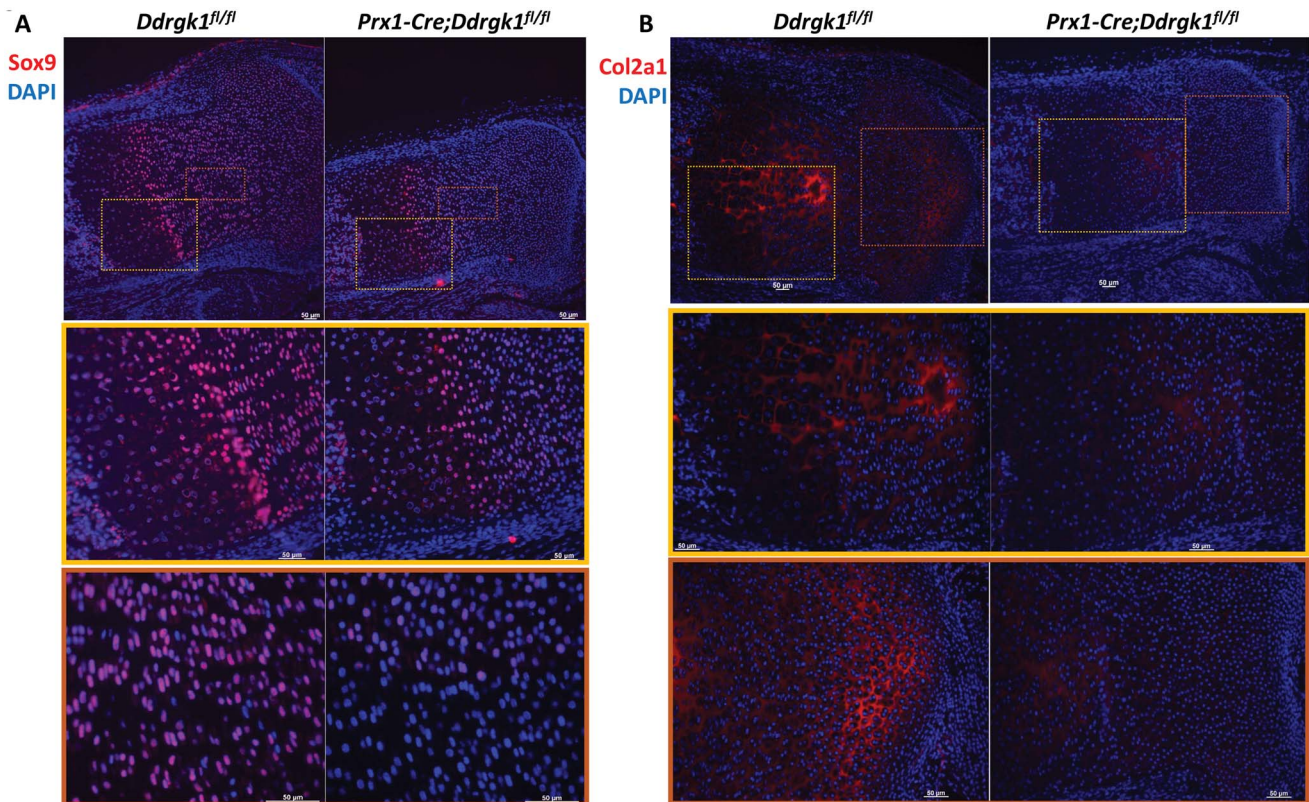
Figure 6. Deletion of *Ddrgk1* causes reduced protein level of Sox9 and Col2a1. (**A**) Sox9 immunofluorescence staining at P2 mice: left panel, *Ddrgk1$^{fl/fl}$* mouse tibia at 10× magnification, 20× magnification of proliferating, prehypertrophic and hypertrophic zones (yellow box), 40× magnification of proliferating zone in growth plates (orange box). Scale bar 50 microns. Right panel: Prx1-Cre; *Ddrgk1$^{fl/fl}$* tibia with same magnification, respectively. (**B**) Col2a1 immunofluorescent staining at P2 mice: left panel, *Ddrgk1$^{fl/fl}$* mouse tibia at 10× magnification, 20× magnification of proliferating, prehypertrophic and hypertrophic zones (yellow box), 20× magnification of resting and proliferating zone in growth plates (orange box). Right *Prx1-Cre; Ddrgk1$^{fl/fl}$* panel: *Prx1-Cre; Ddrgk1$^{fl/fl}$* tibia with same magnification, respectively. Scale bar 50 microns.

To investigate the role of Ddrgk1 in postnatal growth plate cartilage homeostasis, the *Aggrecan Cre^{ERT2}*-inducible mouse model was used in which *Ddrgk1* was deleted at the age of 3 months. Postnatal cartilage-specific conditional deletion of *Ddrgk1* caused widening of the growth plate associated with morphologically enlarged and rounded chondrocytes (Fig. 7). In addition, these findings were associated with significantly reduced proteoglycan staining. In this model, no changes in Col2a1 protein level were observed, but this might be explained by the timing of the deletion induced by tamoxifen. It was shown previously that Sox9 is important for growth plate cartilage homeostasis and that deletion of Sox9 at different postnatal stages causes severe cartilage abnormalities including disruption of the columnar organization of the growth plate, reduced chondrocyte proliferation and abnormal proteoglycan deposition (27). The results of postnatal deletion of *Ddrgk1* found in this study are similar to postnatal *Sox9* deletion including growth plate disorganization and severe abnormalities of proteoglycan deposition. Differences might be explained in part by the later stage deletion of *Ddrgk1*, 3 months instead of 3 weeks that was used in the other study. The reduction in proteoglycan deposition could be secondary to a reduction in proliferating chondrocytes that are the main producers of ECMs. ECM protein deposition is

critical to the development and maintenance of growth and articular cartilage (30–32).

In recent years, mutations in another component of the ufmylation pathway, *UFSP2,* have been associated with autosomal dominant skeletal dysplasia. The first report described a missense mutation in a family with Beukes hip dysplasia (16). More recently, a Di Rocco type SEMD was associated with another missense mutation in *UFSP2* (17,18). DDRGK1 is known to interact with UFSP2 *in vitro* and undergoes de-ufmylation by UFSP2 (5). This interaction occurs at the ER membrane and the localization of UFSP2 at the ER membrane is DDRGK1-dependent (21). The finding that both DDRGK1 and UFSP2 regulate the ufmylation pathway and are associated with SEMD support a specific requirement for ufmylation PTM in chondrogenesis.

In this study, we show for the first time that Ddrgk1, an ufmylation substrate as well as an ufmylation pathway regulator, has a critical role in the organization and maintenance of the growth plate cartilage during development and the postnatal period. We hypothesize that the mechanism underlying SOX9 downregulation in Shohat type SEMD is associated with dysregulation of the ufmylation pathway in developing cartilage. Future studies assessing the role of ufmylation as well as identification of novel ufmylation substrates in chondrogenesis can
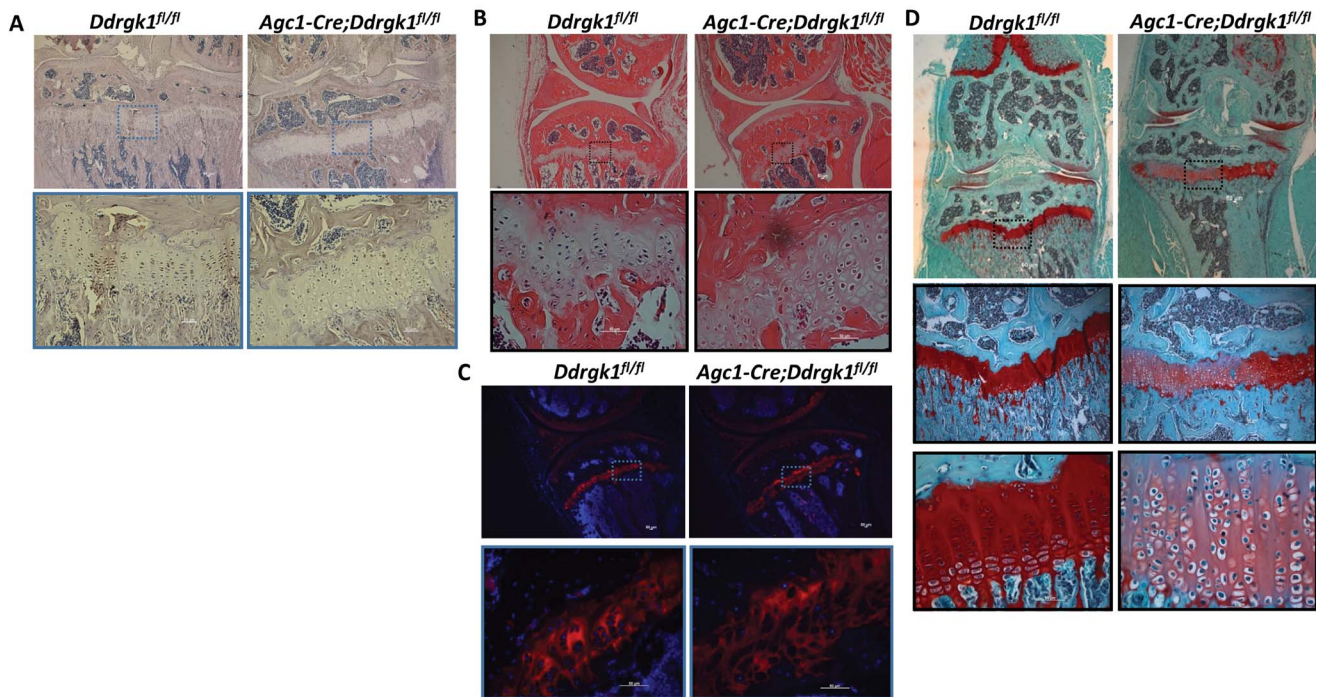
Figure 7. Postnatal *Ddrgk1* deletion causes abnormal growth plate organization. (**A**) Ddrgk1 IHC shows reduced Ddrgk1 expression in the *Agc1-Cre; Ddrgk1*^{fl/fl} mice. Magnification: Upper panel—5×, lower panel—20×. Scale 50 micron. (**B**) H&E staining shows an enlarged chondrocyte morphology with increased cytoplasm. Magnification: upper panel—5×, lower panel—40×. (C) Col2a1 immunofluorescence staining similar Col2a1 staining with widened growth plate in *Agc1-Cre; Ddrgk1*^{fl/fl} mice. Magnification: upper panel—5×, lower panel—40×. Representative slides from $n - 3$. Scale 50 micron. (**D**) SAFO staining (glycoprotein) of hind limb knee joint at 6–month-old males either *Ddrgk1*^{fl/fl} or *Agc1-Cre*^{ERT}; *Ddrgk1*^{fl/fl} after Tamoxifen injection. Reduced glycoprotein staining observed in *Agc1-Cre*^{ERT}; *Ddrgk1*^{fl/fl} mice in addition to altered cellular morphology and widening of the growth plate. Magnification: upper panel—2.5×, middle panel—10×, lower panel—40×. Scale 50 micron.

potentially allow the development of targeted therapies for skeletal dysplasia, especially SEMDs.

Materials and Methods
Animals

Mice were housed in the Baylor College of Medicine vivarium in a pathogen-free environment with ad libitum access to food and water and were maintained under a 14-h light/10-h dark cycle. All studies were approved by the Baylor College of Medicine Institutional Animal Care and Use Committee and Center for Comparative Medicine (protocol number AN-1506). All mice were generated on a C57BL/6 genetic background.

Generation of Prx1-Cre; Ddrgk1^{fl/fl} mice

Conditional *Ddrgk1*^{tm1a(EUCOMM) Hmgu} mice have a Frt-LacZ-loxP-neo-Frt-loxP cassette in between the second and third exons and a loxP site after the fourth exon. These mutant mice were intercrossed with *CMV-Flp* mice, which removed the LazC-neo cassette to generate *CMV-Flp; Ddrgk1*^{fl/fl} mice. The *Flp* allele was bred out by backcrossing *CMV-Flp; Ddrgk1*^{fl/fl} mice to C57/B6J mice. Finally, *Ddrgk1*^{fl/fl} mice were intercrossed with *Prx1-Cre* mice [33] to obtain desired genotypes, which were *Ddrgk1*^{fl/fl} and *Prx1-Cre; Ddrgk1*^{fl/fl} mice.

Generation of Agc1-Cre^{ERT2}; Ddrgk1^{fl/fl} mice

Ddrgk1^{fl/fl} mice described in previous section were intercrossed with *Agc1-Cre*^{ERT} mice [34] to generate second-generation *Agc1-Cre*^{ERT2}; *Ddrgk1*^{fl/fl} mice. Tamoxifen (concentration 20 mg/ml, injected at 1 mg/10 g) was injected for 5 days at age 3 months and mice were collected at 6 months of age.

Generation of OC-Cre; Ddrgk1^{fl/fl} mice

Ddrgk1^{fl/fl} mice described in previous section were intercrossed with *OC-Cre* mice [22] provided generously by Dr Thomas L. Clemens to generate second-generation *OC-Cre; Ddrgk1*^{fl/fl} mice.

Generation of Lepr-Cre; Ddrgk1^{fl/fl} mice

Ddrgk1^{fl/fl} mice described in previous section were intercrossed with *Lepr-Cre; Rosa26-tdTomato*^{fl/fl} [35] mice provided generously by Dr Dongsu Park to generate second-generation *Lepr-Cre; Ddrgk1*^{fl/fl} mice.

Histology and immunohistochemistry

P2 hindlimbs were collected, fixed in 4% PFA at 4°C for 48 h on a shaker and then decalcified in 10% EDTA at 4°C overnight on a shaker. Afterwards, hindlimbs were dehydrated, embedded in paraffin and sectioned 7 μm thick. H&E staining (Sigma, MA 01803 United States) was

used to examine morphology. For immunohistochemistry, slides were deparaffinized and rehydrated. We performed antigen retrieval with 0.05% trypsin for 15 min at 37°. Sample slides were washed with PBS prior to endogenous peroxidase blocking with 3% hydrogen peroxide for 10 min at room temperature. After incubation with blocking solution (Vector-Vectastain ABC kit HRP), we incubated sections with Anti-DDRGK1 (Abcam, Waltham, MA 02453 USA ab99121) for overnight in 4°C. Rabbit IgG secondary antibody was used next day from Vectastain ABC kit and DAB (Vector SK-4100) staining performed per manufacturer instruction. Hematoxylin staining was performed next and mounted using Cytoseal XYL xylene-based mounting medium (Thermo Scientific, Waltham, MA, USA). Images were taken with a light microscope (Axioplan 2, Zeiss) using identical exposure times.

Immunofluorescent staining

Briefly, histology slides were prepared as described in histology section above. Blocking performed with 3% normal serum for 1 h room temperature. After blocking, sample slides were incubated with primary antibody either anti-COL2A1 (Santa Cruz, Dallas, TX, USA M2139), anti-SOX9 (Millipore AB5535) or anti-COL10A1 (DSHB, Iowa City, IA, USA X-AC9) overnight. Secondary antibody either donkey anti-rabbit Alexa Fluor 594 (Invitrogen, Waltham, MA, USA R37119) or goat anti-mouse Alexa Fluor 594 (Invitrogen A21203) pending on the primary antibody were added after PBS wash of the slides and incubated with the antibody for 1 hour.

Alcian blue and Alizarin red staining of skeletal preparation

After removing the skin and organs, P7 pups were in fixed 95% for 24 h at room temperature and then acetone overnight. After the overnight incubation, pups were stained in Alcian blue–Alizarin red solution (0.03% Alcian blue 8GX, 0.005% Alizarin red S type 10% acetic acid and 80% ethanol) for 4 days at room temperature while gently rocking on the shaker. After staining for 4 days, the specimens were placed in 95% ethanol for 6 h and then the skeleton was cleared in 1% KOH for 7–10 days. The clearing solution was gradually replaced with 80% glycerol: 20%.

In vitro osteoblast differentiation assay

Bone marrow stromal cells were collected from 8-week-old *OC-Cre; Ddrgk1$^{fl/fl}$* and control *Ddrgk1$^{fl/fl}$* mice. After removal and cleaning of femurs and tibia, distal end of the bones was removed and bone marrow cells were flushed out by centrifugation at 14 000 rpm for 1 min. Cells were plated in six well plates and grown to confluency in alpha-MEM with 10% FBS media. Osteogenic differentiation was induced with media supplemented with 500 micromolar ascorbic acid (Sigma 255 564) and 5 millimolar BGP (β-glycerophosphate, Sigma G9422) for 21 days. Alizarin red S staining was performed after fixation of cells with 4% formalin.

Bone micro-CT and analysis

Samples were scanned in 70% ethanol at 16 μm resolution using a Scanco micro-CT μCT 40 system. Trabecular and cortical analyses are performed using Scanco analysis software, μCT V6.1. Radiographs performed with the Kubtec XPERT80 (Kubtec X-ray, Milford, CT). Bone parameters, including bone volume, total volume, trabecular number, trabecular thickness and trabecular separation, were measured in the cancellous region of the distal femur by analyzing 75 slides, and cortical thickness was measured by analyzing 50 slides in the femur mid-shaft, except in *Prx1-Cre* line mice where the number of slides analyzed in cko mice was normalized to total femur length.

Quantitative Real-time Polymerase Chain Reaction (qRT-PCR)

Total RNA was extracted from tissues and cells using TRIzol reagent (Invitrogen) and cDNA was synthesized from total RNA using the SuperScript III First Strand RT-PCR kit (Invitrogen). The qRT-PCR was performed on a Light-Cycler instrument (Roche). Murine β-actin or Gapdh was used as the internal control to normalize gene expression.

Primers

Ddrgk1$^{fl/fl}$ forward	TGCCCGGCTGTCTGTCGTC
Ddrgk1$^{fl/fl}$ reverse	TACCAAAGCCCAGGAACTCT
Cre forward	TCCAATTTACTGACCGTACACCAA
Cre reverse	CCTGATCCTGGCAATTTCGGCTA
Ddrgk1 exon3 forward	ATTGAGAAGCCAGCAGAAGTTCACCC
Ddrgk1 exon3 reverse	TGAGCCTTTCGAGCCTGTTTTTCCTCTA
Ddrgk1 exon 9 forward	CGACCGGGGCAAGTTTATCTAC
Ddrgk1 exon 9 reverse	ACGGCATTAGGGAAGGATGAAGACAC
mGAPDH forward	GCAAGAGAGGCCCTATCCCAA
mGAPDH reverse	CTCCCTAGGCCCCTCCTGTTATT

Statistical analyses

All statistical analyses used parametric unpaired tests including one-way analysis of variance or *t*-tests. Prism-9 GraphPad (https://www.graphpad.com/scientific-software/prism/) was used to help with statistical analysis. *P*-values <0.05 were considered significant.

Supplementary Material

Supplementary Material is available at *HMG* online.

Conflict of Interest statement. The authors declare that they have no conflict of interest related to this work.

Funding

References

1. Costantini, A., Muurinen, M.H. and Makitie, O. (2021) New gene discoveries in skeletal diseases with short stature. *Endocr. Connect.*, **10**, R160–r174.

2. Cormier-Daire, V. (2008) Spondylo-epi-metaphyseal dysplasia. *Best Pract. Res. Clin. Rheumatol.*, **22**, 33–44.

3. Mortier, G.R., Cohn, D.H., Cormier-Daire, V., Hall, C., Krakow, D., Mundlos, S., Nishimura, G., Robertson, S., Sangiorgi, L., Savarirayan, R. *et al.* (2019) Nosology and classification of genetic skeletal disorders: 2019 revision. *Am. J. Med. Genet. A*, **179**, 2393–2419.

4. Komatsu, M., Chiba, T., Tatsumi, K., Iemura, S., Tanida, I., Okazaki, N., Ueno, T., Kominami, E., Natsume, T. and Tanaka, K. (2004) A novel protein-conjugating system for Ufm1, a ubiquitin-fold modifier. *EMBO J.*, **23**, 1977–1986.

5. Tatsumi, K., Sou, Y.S., Tada, N., Nakamura, E., Iemura, S., Natsume, T., Kang, S.H., Chung, C.H., Kasahara, M., Kominami, E. *et al.* (2010) A novel type of E3 ligase for the Ufm1 conjugation system. *J. Biol. Chem.*, **285**, 5417–5427.

6. Liu, Y., Molchanov, V. and Yang, T. (2021) Enzymatic machinery of ubiquitin and ubiquitin-like modification systems in chondrocyte homeostasis and osteoarthritis. *Curr. Rheumatol. Rep.*, **23**, 62.

7. Lefebvre, V., Angelozzi, M. and Haseeb, A. (2019) SOX9 in cartilage development and disease. *Curr. Opin. Cell Biol.*, **61**, 39–47.

8. Ba, C., Ni, X., Yu, J., Zou, G. and Zhu, H. (2020) Ubiquitin conjugating enzyme E2 M promotes apoptosis in osteoarthritis chondrocytes via Wnt/beta-catenin signaling. *Biochem. Biophys. Res. Commun.*, **529**, 970–976.

9. Egunsola, A.T., Bae, Y., Jiang, M.M., Liu, D.S., Chen-Evenson, Y., Bertin, T., Chen, S., Lu, J.T., Nevarez, L., Magal, N. *et al.* (2017) Loss of DDRGK1 modulates SOX9 ubiquitination in spondyloepimetaphyseal dysplasia. *J. Clin. Invest.*, **127**, 1475–1484.

10. Akiyama, H., Kamitani, T., Yang, X., Kandyil, R., Bridgewater, L.C., Fellous, M., Mori-Akiyama, Y. and de Crombrugghe, B. (2005) The transcription factor Sox9 is degraded by the ubiquitin-proteasome system and stabilized by a mutation in a ubiquitin-target site. *Matrix Biol.*, **23**, 499–505.

11. Huang, W., Zhou, X., Lefebvre, V. and de Crombrugghe, B. (2000) Phosphorylation of SOX9 by cyclic AMP-dependent protein kinase A enhances SOX9's ability to transactivate a Col2a1 chondrocyte-specific enhancer. *Mol. Cell. Biol.*, **20**, 4149–4158.

12. Feng, D., Kang, X., Wang, R., Chen, H., Zhang, K., Feng, W., Li, H., Zhu, Y. and Wu, S. (2020) Progranulin modulates cartilage-specific gene expression via sirtuin 1-mediated deacetylation of the transcription factors SOX9 and P65. *J. Biol. Chem.*, **295**, 13640–13650.

13. Bar Oz, M., Kumar, A., Elayyan, J., Reich, E., Binyamin, M., Kandel, L., Liebergall, M., Steinmeyer, J., Lefebvre, V. and Dvir-Ginzberg, M. (2016) Acetylation reduces SOX9 nuclear entry and ACAN gene transactivation in human chondrocytes. *Aging Cell*, **15**, 499–508.

14. Saotome, H., Ito, A., Kubo, A. and Inui, M. (2020) Generation of a quantitative luciferase reporter for Sox9 SUMOylation. *Int. J. Mol. Sci.*, **21**, 1274.

15. Hattori, T., Eberspaecher, H., Lu, J., Zhang, R., Nishida, T., Kahyo, T., Yasuda, H. and de Crombrugghe, B. (2006) Interactions between PIAS proteins and SOX9 result in an increase in the cellular concentrations of SOX9. *J. Biol. Chem.*, **281**, 14417–14428.

16. Watson, C.M., Crinnion, L.A., Gleghorn, L., Newman, W.G., Ramesar, R., Beighton, P. and Wallis, G.A. (2015) Identification of a mutation in the ubiquitin-fold modifier 1-specific peptidase 2 gene, UFSP2, in an extended South African family with Beukes hip dysplasia. *S. Afr. Med. J.*, **105**, 558–563.

17. Di Rocco, M., Rusmini, M., Caroli, F., Madeo, A., Bertamino, M., Marre-Brunenghi, G. and Ceccherini, I. (2018) Novel spondyloepimetaphyseal dysplasia due to UFSP2 gene mutation. *Clin. Genet.*, **93**, 671–674.

18. Zhang, G., Tang, S., Wang, H., Pan, H., Zhang, W., Huang, Y., Kong, J., Wang, Y., Gu, J. and Wang, Y. (2020) UFSP2-related spondyloepimetaphyseal dysplasia: a confirmatory report. *Eur. J. Med. Genet.*, **63**, 104021.

19. Shohat, M., Lachman, R., Carmi, R., Bar Ziv, J. and Rimoin, D. (1993) New form of spondyloepimetaphyseal dysplasia (SEMD) in Jewish family of Iraqi origin. *Am. J. Med. Genet.*, **46**, 358–362.

20. Ishimura, R., Obata, M., Kageyama, S., Daniel, J., Tanaka, K. and Komatsu, M. (2017) A novel approach to assess the ubiquitin-fold modifier 1-system in cells. *FEBS Lett.*, **591**, 196–204.

21. Ha, B.H., Jeon, Y.J., Shin, S.C., Tatsumi, K., Komatsu, M., Tanaka, K., Watson, C.M., Wallis, G., Chung, C.H. and Kim, E.E. (2011) Structure of ubiquitin-fold modifier 1-specific protease UfSP2. *J. Biol. Chem.*, **286**, 10248–10257.

22. Zhang, M., Xuan, S., Bouxsein, M.L., von Stechow, D., Akeno, N., Faugere, M.C., Malluche, H., Zhao, G., Rosen, C.J., Efstratiadis, A. *et al.* (2002) Osteoblast-specific knockout of the insulin-like growth factor (IGF) receptor gene reveals an essential role of IGF signaling in bone matrix mineralization. *J. Biol. Chem.*, **277**, 44005–44012.

23. DeFalco, J., Tomishima, M., Liu, H., Zhao, C., Cai, X., Marth, J.D., Enquist, L. and Friedman, J.M. (2001) Virus-assisted mapping of neural inputs to a feeding center in the hypothalamus. *Science*, **291**, 2608–2613.

24. Hoggard, N., Hunter, L., Lea, R.G., Trayhurn, P. and Mercer, J.G. (2000) Ontogeny of the expression of leptin and its receptor in the murine fetus and placenta. *Br. J. Nutr.*, **83**, 317–326.

25. Zhou, B.O., Yue, R., Murphy, M.M., Peyer, J.G. and Morrison, S.J. (2014) Leptin-receptor-expressing mesenchymal stromal cells represent the main source of bone formed by adult bone marrow. *Cell Stem Cell*, **15**, 154–168.

26. Akiyama, H., Chaboissier, M.C., Martin, J.F., Schedl, A. and de Crombrugghe, B. (2002) The transcription factor Sox9 has essential roles in successive steps of the chondrocyte differentiation pathway and is required for expression of Sox5 and Sox6. *Genes Dev.*, **16**, 2813–2828.

27. Henry, S.P., Liang, S., Akdemir, K.C. and de Crombrugghe, B. (2012) The postnatal role of Sox9 in cartilage. *J. Bone Miner. Res.*, **27**, 2511–2525.

28. Wei, Y. and Xu, X. (2016) UFMylation: a unique & fashionable modification for life. *Genomics Proteomics Bioinformatics*, **14**, 140–146.

29. Herhaus, L. and Dikic, I. (2015) Expanding the ubiquitin code through post-translational modification. *EMBO Rep.*, **16**, 1071–1083.

30. Schwartz, N.B. and Domowicz, M. (2002) Chondrodysplasias due to proteoglycan defects. *Glycobiology*, **12**, 57R–68R.

31. Domowicz, M.S., Cortes, M., Henry, J.G. and Schwartz, N.B. (2009) Aggrecan modulation of growth plate morphogenesis. *Dev. Biol.*, **329**, 242–257.

32. Lauing, K.L., Cortes, M., Domowicz, M.S., Henry, J.G., Baria, A.T. and Schwartz, N.B. (2014) Aggrecan is required for growth plate cytoarchitecture and differentiation. *Dev. Biol.*, **396**, 224–236.

33. Logan, M., Martin, J.F., Nagy, A., Lobe, C., Olson, E.N. and Tabin, C.J. (2002) Expression of Cre recombinase in the developing mouse limb bud driven by a Prxl enhancer. *Genesis*, **33**, 77–80.

34. Henry, S.P., Jang, C.W., Deng, J.M., Zhang, Z., Behringer, R.R. and de Crombrugghe, B. (2009) Generation of aggrecan-CreERT2 knockin mice for inducible Cre activity in adult cartilage. *Genesis*, **47**, 805–814.

35. Ortinau, L.C., Wang, H., Lei, K., Deveza, L., Jeong, Y., Hara, Y., Grafe, I., Rosenfeld, S.B., Lee, D., Lee, B. *et al.* (2019) Identification of functionally distinct Mx1+alphaSMA+ periosteal skeletal stem cells. *Cell Stem Cell*, **25**, 784, e785–796.